

Exercise 1 - Trajectory of rotating ball

Tom Vadot, Martin Godet

tom.vadot@epfl.ch, martin.godet@epfl.ch

March 4, 2024

Contents

1	Introduction	1
2	Analytical results	2
2.1	System of differential equations	2
2.2	Mechanical energy	2
2.3	Zero-gravity situation	3
2.4	Gravity with no initial speed situation	4
3	Simulations	5
3.1	Rotating ball in zero gravity	5
3.1.1	Numeric convergence	6
3.1.2	Numeric stability	6
3.2	Rotating ball with gravity	7
3.2.1	Method comparison	7
3.2.2	Adding drag force	9
4	Conclusion	10

1 Introduction

In this paper we aim at giving a comprehensive numerical analysis of a typical case study, the trajectory of a rotating ball under the influence of the Magnus effect. This analysis will be done using three related types of algorithms: Euler explicit, implicit and semi-implicit. Their numerical convergence and stability will be studied in the various cases where they have been used.

The algorithms used will be implemented through a C++ simulation and the obtained data analysed using classic python libraries. The first simulation will show what happens if a rotating ball is given an initial velocity in a zero gravity environment. The second simulation will have two different iterations of the same situation, a rotating ball being released with zero velocity in a gravity field. The first iteration will show how, when not accounting for air drag, the ball eventually goes back to its original height and enters a periodic process. The second will account for air drag and analyse the deflected trajectory. Some analytical results will also be proven in order to verify the soundness of our simulation by comparing them to the computational results.

2 Analytical results

For the purpose of this study it is first needed to prove some analytical results that will later be achieved through numerical simulations.

We are considering a sphere (tennis ball) of mass m and radius R . It is rotating according to $\vec{\omega} = \omega \vec{e}_z$. It is moving in the gravity field $\vec{g} = -g \vec{e}_y$ and inside a fluid of density ρ which applies a force due to the Magnus effect:

$$\vec{F}_p = \mu R^3 \rho \vec{\omega} \times \vec{v} \quad (1)$$

We want to determine the movement of the ball knowing the initial velocity \vec{v}_0 and rotation $\vec{\omega}$. In an effort to simplify the problem we assume that the rotation is constant and we consider trajectories occuring only on the (x, y) plane.

2.1 System of differential equations

Question 1.1-(a)

Let us take the vector: $\mathbf{y} = (x, y, v_x, v_y)$

We are searching for f such that:

$$\frac{d\mathbf{y}}{dt} = \begin{pmatrix} v_x \\ v_y \\ a_x \\ a_y \end{pmatrix} = f(\mathbf{y}) \quad (2)$$

We know that $m\vec{a} = \vec{F}_p + m\vec{g}$ and from EQUATION 1 we have:

$$\vec{F}_p = \mu R^3 \rho \omega \begin{pmatrix} -v_y \\ v_x \\ 0 \end{pmatrix}$$

We get from this and $g_z = 0$ that $a_z = 0$ so the trajectory will indeed stay inside the (x, y) plane for $v_z(0) = 0$ and $z(0) = 0$. Most importantly we also get:

$$\begin{pmatrix} a_x \\ a_y \end{pmatrix} = \begin{pmatrix} -\frac{\mu R^3 \rho \omega}{m} v_y \\ \frac{\mu R^3 \rho \omega}{m} v_x - g \end{pmatrix}$$

Which allows us to rewrite EQUATION 2 as:

$$\frac{d\mathbf{y}}{dt} = f(\mathbf{y}) = \begin{pmatrix} v_x \\ v_y \\ -\frac{\mu R^3 \rho \omega}{m} v_y \\ \frac{\mu R^3 \rho \omega}{m} v_x - g \end{pmatrix} \quad (3)$$

2.2 Mechanical energy

Question 1.1-(b)

We are searching for the total mechanical energy of the system. We know that for a rigid body such as the tennis ball considered in this problem the total mechanical energy is the sum of the translational kinetic energy, the rotational kinetic energy and the potential so:

$$E_{\text{tot}} = \frac{1}{2}mv^2 + \frac{1}{2}I\omega^2 + mgy$$

We get the moment of inertia of a sphere for any rotation around an axis going through the center: $I = \frac{2}{5}mR^2$ [1].

Which yields the final formula for the energy:

$$E_{\text{tot}} = \frac{1}{2}mv^2 + \frac{1}{5}mR^2\omega^2 + mgy \quad (4)$$

We now want to know if this energy is conserved. We know that the gravitational force from the \vec{g} field is conservative. We now consider the force \vec{F}_p . It is strictly orthogonal to the velocity at any point from EQUATION 1 which means that \vec{F}_p does not produce any work throughout the movement. We can conclude that we have no non-conservative forces doing work so the total mechanical energy must be conserved.

2.3 Zero-gravity situation

Question 1.1-(c)

All the considerations in this subsection will be done inside the (x, y) plane since we have shown that the movement always stays inside of it. The z and v_z coordinates are thus always 0.

We now want to solve EQUATION 3 for $\vec{g} = 0$ and the initial conditions $\vec{x}(0) = 0$ and $\vec{v}(0) = v_0\vec{e}_x$. Let us write $\alpha = \frac{\mu R^3 \rho \omega}{m}$. We have:

$$a_x = \dot{v}_x = -\alpha v_y \quad (5)$$

$$a_y = \dot{v}_y = \alpha v_x \quad (6)$$

Taking the time derivative yields:

$$\ddot{v}_x = -\alpha \dot{v}_y = -\alpha^2 v_x \implies \ddot{v}_x + \alpha^2 v_x = 0 \quad (7)$$

which we recognise as the harmonic oscillator equation. Its general solution is:

$$v_x(t) = A \cos(\alpha t + \varphi) \quad (8)$$

We can deduce the general solution for $x(t)$ from this:

$$x(t) = \frac{A}{\alpha} \sin(\alpha t + \varphi) + c_1 \quad (9)$$

We can find $y(t)$ by substituting v_x into EQUATION 6

$$\begin{aligned} \dot{v}_y(t) &= \alpha v_x = A\alpha \cos(\alpha t + \varphi) \\ \implies v_y(t) &= A \sin(\alpha t + \varphi) + c_2 \end{aligned} \quad (10)$$

$$\implies y(t) = -\frac{A}{\alpha} \cos(\alpha t + \varphi) + c_2 t + c_3 \quad (11)$$

Using the mentioned initial conditions inside these equations gives us 5 unknowns for 4 equations. For symmetry reasons we can set $\varphi = 0$ which gives the other constants:

$$c_1 = 0, \quad c_2 = 0, \quad c_3 = \frac{v_0}{\alpha}, \quad A = v_0$$

We now want to characterise the type of movement we are having with this ball. We show that the acceleration is orthogonal to the velocity and has a constant norm:

$$\vec{a} \cdot \vec{v} = \alpha(-v_y v_x + v_x v_y) = 0 \quad (12)$$

$$||\vec{a}||^2 = \alpha^2((-v_y)^2 + (v_x)^2) = \alpha^2 A^2 = \text{cst} \quad (13)$$

This means that the movement is circular uniform and we can write:

$$\begin{aligned} a &= \frac{v^2}{r}, \quad a = \alpha v_0, \quad v = \text{cst} = v_0 \\ &\Rightarrow r = \frac{v_0}{\alpha} \end{aligned} \quad (14)$$

with r the radius of the circular movement. The angular frequency is given by: $\Omega = \frac{v}{r} = \alpha$.

For clarity we rewrite EQUATION 8 to 11 with the constants found and reminding that $\alpha = \frac{\mu R^3 \rho \omega}{m}$:

$$\begin{cases} x(t) = \frac{v_0}{\alpha} \sin(\alpha t) \\ y(t) = \frac{v_0}{\alpha} (1 - \cos(\alpha t)) \\ v_x(t) = v_0 \cos(\alpha t) \\ v_y(t) = v_0 \sin(\alpha t) \end{cases} \quad (15)$$

2.4 Gravity with no initial speed situation

Question 1.1-(d)

We now want to solve the same problem with $g \neq 0$. The given initial conditions are $\vec{x}(0) = 0$ and $\vec{v}(0) = 0$.

We choose a new referential \mathcal{R}' moving at a constant velocity $\vec{v}_E = \frac{m}{\omega^2 \mu R^3 \rho} \vec{\omega} \times \vec{g} = \frac{1}{\alpha} \vec{e}_z \times \vec{g}$ relative to our first referential \mathcal{R} .

We first write down the equations of motion in the new referential using $\vec{v} = \vec{v}' + \vec{v}_E \Rightarrow \vec{a} = \vec{a}'$:

$$\begin{aligned} \vec{a}' &= \frac{1}{m} \vec{F}_p + \vec{g} \\ &= \alpha \vec{e}_z \times \vec{v} + \vec{g} \\ &= \alpha \vec{e}_z \times \vec{v}' + \alpha \vec{e}_z \times \vec{v}_E + \vec{g} \\ &= \alpha \vec{e}_z \times \vec{v}' + \vec{e}_z \times (\vec{e}_z \times \vec{g}) + \vec{g} \\ &= \alpha \vec{e}_z \times \vec{v}' + g(-\vec{e}_z \times (\vec{e}_z \times \vec{e}_y) - \vec{e}_y) \\ &= \alpha \vec{e}_z \times \vec{v}' + g(\vec{e}_y - \vec{e}_y) \\ &\Rightarrow \vec{a}' = \alpha \begin{pmatrix} -v'_y \\ v'_x \\ 0 \end{pmatrix} \end{aligned} \quad (16)$$

In the question 1.1-(c) we had an equation of motion $\vec{a} = \alpha \vec{e}_z \times \vec{v}$ which has the exact same form and thus the general solutions are the same for \vec{a}' and \vec{v}' as in EQUATION 8 to 11.

Assuming like before $\varphi = 0$ and using the given initial conditions we can find:

$$A = -v_E, \quad c_3 = -\frac{v_E}{\alpha}, \quad c_1 = 0, \quad c_2 = 0$$

with $v_E = \frac{g}{\alpha} \vec{e}_x$.

This gives us our final solution by changing back to the \mathcal{R} referential knowing it will have translated along \hat{x} by $x = x' + v_E t$:

$$\begin{cases} x(t) = -\frac{g}{\alpha^2} \sin(\alpha t) + \frac{g}{\alpha} t \\ y(t) = \frac{g}{\alpha^2} (\cos(\alpha t) - 1) \end{cases} \quad (17)$$

We want to determine if the ball will at some point get back to its starting height $y = 0$. We see easily that the movement according to y is periodic with a cosine being the only term depending on t . More formally, because \cos is 2π -periodic, we have for $t_{\text{fin}} = 2\pi/\alpha$:

$$y(t_{\text{fin}}) = \frac{g}{\alpha^2} \left(\cos\left(\frac{2\pi\alpha}{\alpha}\right) - 1 \right) = \frac{g}{\alpha^2} (1 - 1) = 0$$

which does show that at $t_{\text{fin}} = 2\pi/\alpha = 2\pi m / \mu R^3 \rho \omega$ the ball gets back to its original height. This happens at a distance L from the origin:

$$\begin{aligned} L = x(t_{\text{fin}}) &= -\frac{g}{\alpha^2} \sin\left(\frac{2\pi\alpha}{\alpha}\right) + \frac{2\pi g}{\alpha^2} \\ L &= \frac{2\pi g}{\alpha^2} = \frac{2\pi g m^2}{(\mu R^3 \rho \omega)^2} \end{aligned} \quad (18)$$

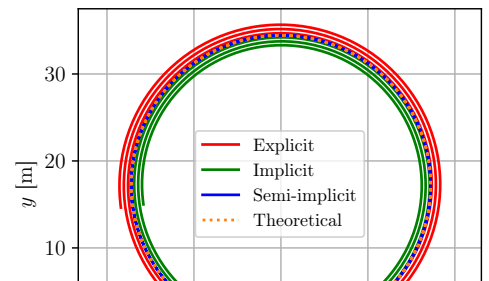
3 Simulations

3.1 Rotating ball in zero gravity

The simulations were done on a tennis ball of mass $m = 0.056$ kg and radius $R = 0.033$ m, with air density $\rho = 1.2$ kg/m³. The coefficient $\mu = 6$ has been chosen. The ball is sent with initial conditions $\omega = 10$ rotations/s ($\omega = 20\pi$ rad/s), $\vec{x}(0) = \vec{0}$, $\vec{v}(0) = 5\vec{e}_x$ and its trajectory is simulated until $t_{\text{fin}} = 60$ s.

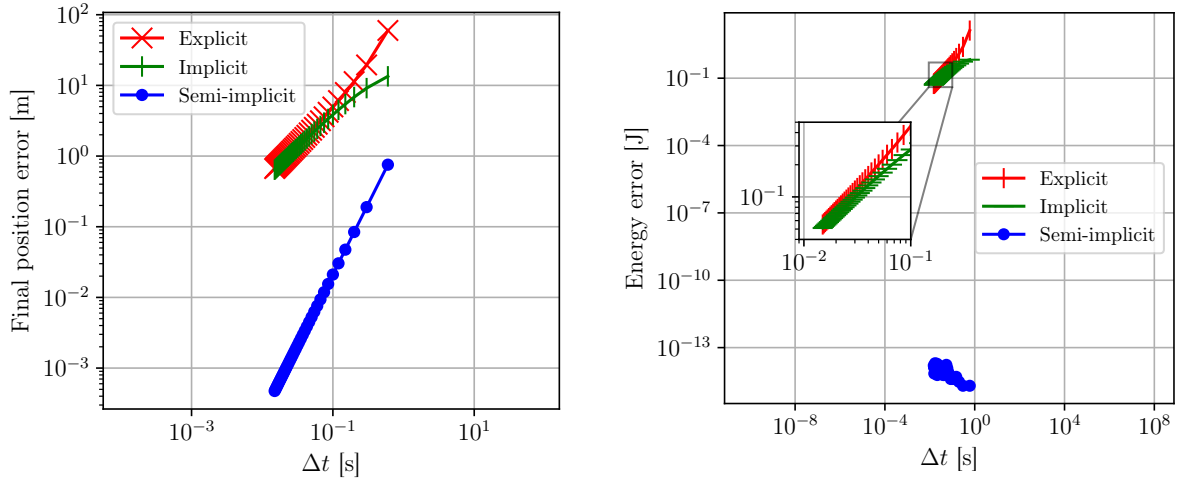
To lighten the notation, we will use EE for the Explicit Euler method, IE for Implicit Euler and SE for Semi-implicit Euler.

The position after t_{fin} is shown in FIGURE 1. We can see that the EE method overshoots the expected trajectory, while the IE method undershoots it and SE remains almost exactly on the analytical result.



3.1.1 Numeric convergence

The numeric convergence of the final position of each method is illustrated in FIGURE 2A. We observe that the error on the final position tends to 0 as $\Delta t \rightarrow 0$ for every method, meaning that they all converge numerically. Furthermore, the convergence order is given by the slope of the line passing through the points. We can thus deduce that the convergence order is 1 for EE and IE, and 2 for SE.



(a) Error on final position w.r.t. analytical solution. n_{steps} was varied between 100 and 4000.

(b) Error on final energy for each method where the error is defined as $\max(E_{\text{mec}}) - \min(E_{\text{mec}})$. (maximum $n_{\text{steps}} = 4000$)

Figure 2: Numeric convergence analysis for different methods

The numeric convergence of the energy for each method is also given in FIGURE 2B. Again, we observe that the error clearly tends to 0, as $\Delta t \rightarrow 0$ for EE and IE. The error for SE remains quite constant and is of the order of 10^{-14} , close to the limit for double-precision floating point numbers. We thus conclude that every method converges numerically. The convergence order for EE and IE is 1, but SE does not have a convergence order as its energy remains pretty much constant for a wide range of Δt .

3.1.2 Numeric stability

To illustrate the numeric stability of each method, the energy over time has been plotted in FIGURE 3. EE is numerically unstable, as its energy over time grows exponentially for smaller n_{steps} . IE is stable, but loses energy over time, decaying exponentially. Using a curve fit of the function $g(t) = A + e^{\gamma t}$, where A is an offset and γ is the growth rate, to calculate the growth or decrease rate we obtain the results presented in TABLE 1. Finally, the SE method remains at constant energy even for smaller n_{steps} , meaning it is both stable and conserves energy.

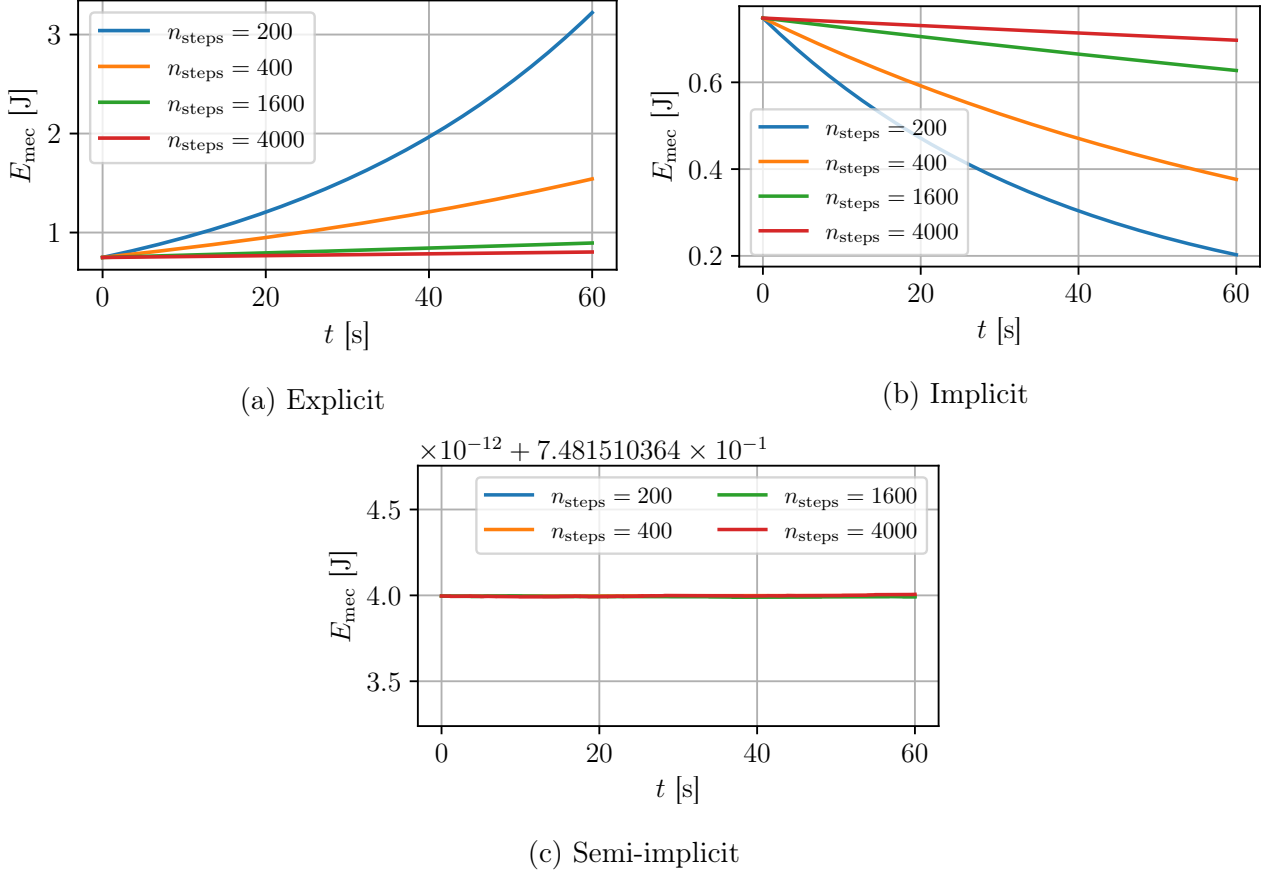


Figure 3: Energy over time for different methods and n_{steps} . To improve the results, the tolerance on the error was set to 10^{-10}

n_{steps}	200	400	1600	4000
EE	0.0203	0.0096	0.0023	0.0009
IE	-0.0146	-0.0081	-0.0022	-0.0009

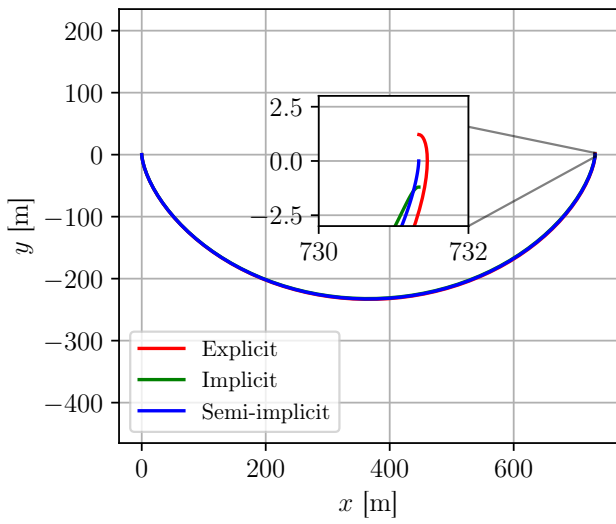
Table 1: Rate of growth or decrease for non energy-conserving methods

3.2 Rotating ball with gravity

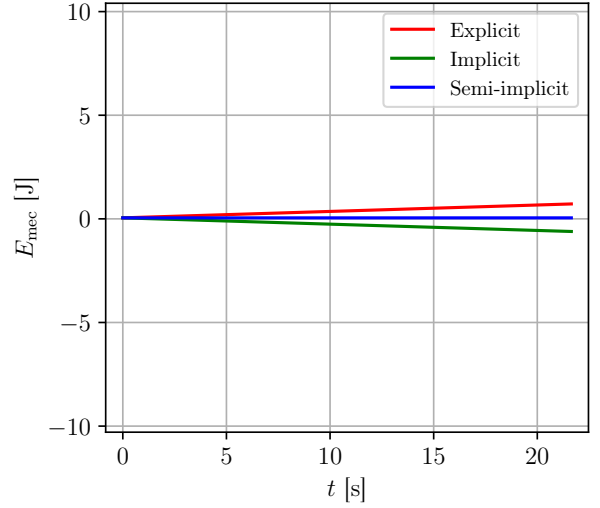
3.2.1 Method comparison

Another set of simulations was run with $\vec{g} = -9.81\vec{e}_y$ to analyse a more realistic trajectory. The tennis ball is let go at $\vec{x}(0) = \vec{0}$ and with $\vec{v}(0) = \vec{0}$. It rotates with the same angular speed ω as in the previous part. The simulation was run up to the time t_{fin} calculated in SUBSECTION 2.4 for the numerical values given. The given results for trajectories and energy are shown respectively in FIGURE 4A and FIGURE 4B.

The trajectories obtained are extremely similar and diverge slightly around the end of the simulation as the close-up view shows. The expected behavior is observed with EE slightly overshooting, having gained energy, and IE falling short of reaching the original height of $y(0) = 0$ with a loss of energy. As before, the SE method is extremely precise, ending up exactly at the expected height at the time of the end of the simulation corresponding to the theoretical value.



(a) Trajectories of the falling ball with each method



(b) Evolution of the energy of the simulation for each method

Figure 4: Simulation of the falling tennis ball with the three methods EE, IE and SE ($n_{\text{steps}} = 2000$)

In particular the FIGURE 4B shows the great stability of the SE method with an energy seemingly constant. The EE and IE are more unstable with the energies diverging exponentially from the theoretically constant value. This can be illustrated by observing the trajectories for larger times as shown in FIGURE 5 with $t_{\text{fin}} = 300$ s. In this new simulation it is obvious that the EE diverges strongly. Observing the IE it can also be seen that the amplitude of its oscillations diminish through time as it loses energy.

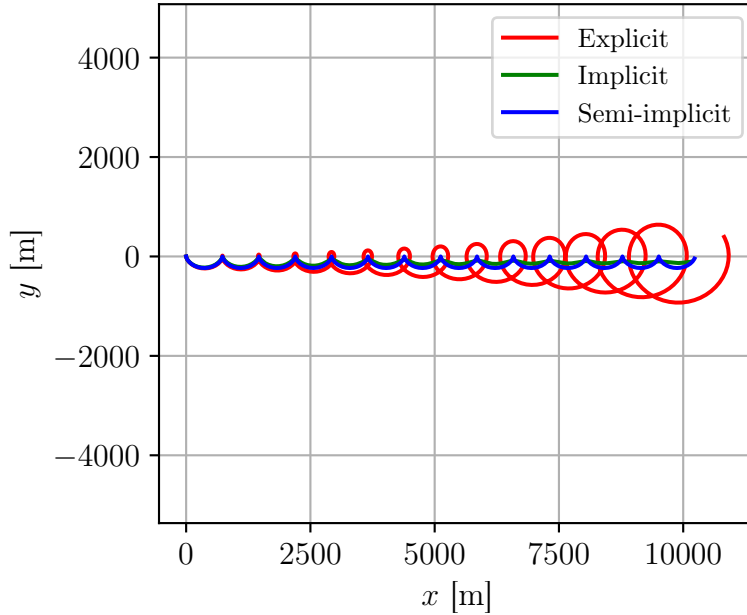
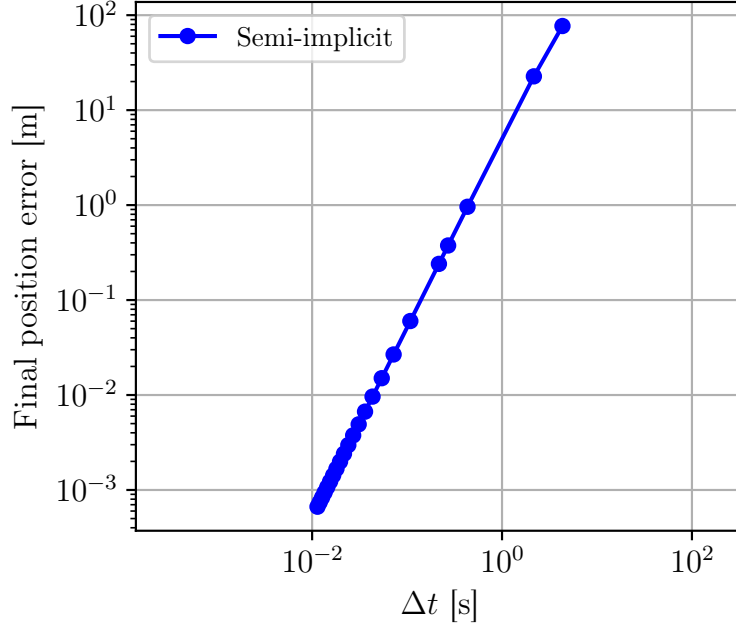
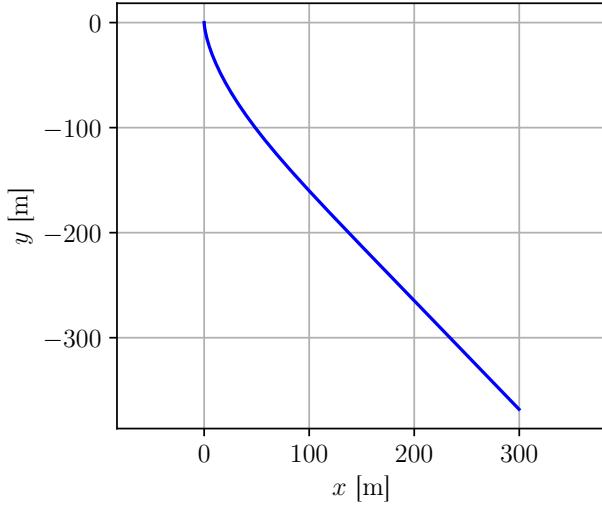


Figure 5: Trajectories for the falling tennis ball with each method for $t_{\text{fin}} = 300$ s

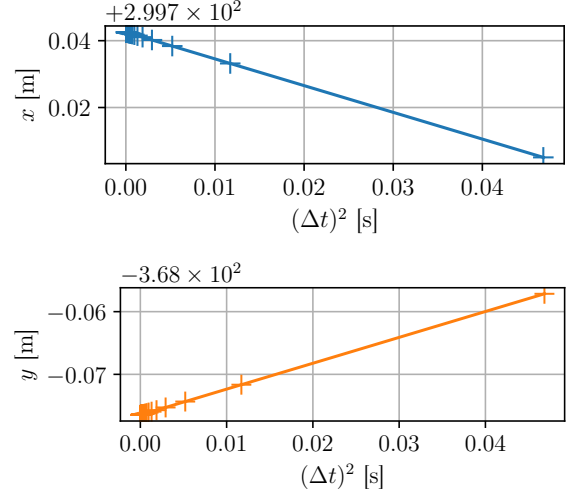
The SE method as been shown to give better results than the other two in this simulation as well. It can also be of interest to determine its order of convergence. As shown in FIGURE 6 the error tends to 0 as $\Delta t \rightarrow 0$ meaning this method converges numerically. The figure is represented

with a log-log scale which allows to read the order of convergence for the SE method is $n = 2$.





(a) Trajectory after t_{fin} ($n_{\text{steps}} = 4000$)



(b) Convergence analysis for the final position. n_{steps} was varied between 100 and 4000.

Figure 7: Simulation of the system including air drag using the SE method

4 Conclusion

Through this report, we learned the differences between the EE, IE, and SE methods and analysed their numerical convergence and stability under different conditions. While the EE and IE methods drifted off the analytical solution, the SE method remained very close to it. It was also notable that the energy of the EE increased exponentially meaning that this method is highly unstable while the IE and SE methods did not have this problem. The physical take away from this analysis is that assuming the absence of air drag can have a major impact on the final results with one situation showing a periodic behavior near the starting height and the other being a deflected fall.

References

- [1] Dr.Peter Dourmashkin. *Moment of Inertia of a Sphere*. URL: <https://ocw.mit.edu/courses/8-01sc-classical-mechanics-fall-2016/resources/29-4/> (visited on 02/25/2024).